Journal of Geochemical Exploration 159 (2015) 243–251

Contents lists available at ScienceDirect

Journal of Geochemical Exploration

journal homepage: www.elsevier.com/locate/jgeoexp

A methodology for wavelength dispersive electron probe microanalysis of unpolished silicate minerals

S. Timmerman [a,*], S. Matveev [a,b], M.U. Gress [a], G.R. Davies [a]

[a] Geology and Geochemistry cluster, VU University, Amsterdam, De Boelelaan 1085, 1081HV Amsterdam, The Netherlands
[b] Department of Petrology, Utrecht University, Heidelberglaan 8, 3584CS Utrecht, The Netherlands

ARTICLE INFO

Article history:
Received 27 March 2015
Revised 4 September 2015
Accepted 23 September 2015
Available online 26 September 2015

Keywords:
Electron microprobe
Wavelength dispersive analysis
Unpolished
Silicate minerals
Rough

ABSTRACT

Evaluation of mineral compositions is a widely used approach in resource exploration strategies where preparation time and cost may prove to be an important factor. In research institutes it is highly beneficial to determine the major element composition of minerals prior to their destructive analysis for trace elements and radiogenic isotopic ratios thus allowing a comprehensive interpretation of mineral petrogenesis. For the analysis of unique and small (submilligram) samples, avoiding sample loss is a key issue in ultimately producing high quality geochemical data. Consequently here we evaluate the precision and accuracy of electron probe microanalysis of unpolished garnet, olivine, orthopyroxene and clinopyroxene grains by comparison of analyses performed on polished thin sections of the same minerals. By utilizing a protocol that focuses on flat mineral surfaces, rejects analyses with low totals (<90%) and major element compositions, magnesium numbers and stoichiometry outside two standard deviation, results had on average a reproducibility of 1.3 times the relative standard deviation of the results of polished thin sections. Major element ratios are indistinguishable from the thin section results. For example, the Mg# for clinopyroxene and olivine is within 0.4% and for garnet within 1–1.5%. Individual analyses of minerals with flat surfaces such as clinopyroxene had a higher rate of success (73%) than minerals with a more variable surface topography such as conchoidally fractured garnet (40%), underlining that a flat topography is the controlling factor in EPMA analyses. These tests establish that accurate and reproducible EPMA analysis can be produced on unpolished minerals that are within error of conventional thin section analyses. The technique is predicted to be of particular use in diamond exploration strategies where knowledge of the geotherm beneath exploration areas is a key parameter. Integrated studies of composition and geochronology of mineral inclusions in diamonds have the potential to significantly improve the understanding of diamond formation processes and the imposed octahedral morphology of the inclusions mean that they have flat crystal faces, ideal for analysis using the proposed methodology.

© 2015 Elsevier B.V. All rights reserved.

1. Introduction

Modern diamond exploration strategies use airborne geophysical techniques to recognize igneous bodies that may represent pyroclastic diatreme deposits (Macnae, 1979). Once potential deposits are recognized on a regional scale, exploration tends to focus on the chemical composition and age of heavy minerals such as garnet, ilmenite and clinopyroxene recovered from drill and soil samples (Coker, 2010). The aim of this strategy is to understand the nature and depth of origin of potential source rocks: i.e., if garnet harzburgite, garnet lherzolite, eclogite etc. are derived from above or below the diamond-graphite phase transition (Averill, 2001; Griffin and Ryan, 1995). The characterization of the rare mineral inclusions found in diamonds using multiple analytical techniques could potentially form an important part of this strategy by helping to define the past regional geothermal gradient and hence the depth range from which diamonds could be sampled by the host volcanic rocks (Grütter et al., 2004; Gurney et al., 2005). Currently, however, the study of such inclusions is rarely incorporated into the exploration strategy, partly due to their small size (typically <100 μm) and the inability to date the inclusions. Recent advances in analytical techniques now make it possible to determine trace element concentrations and radiogenic isotopic ratios on subnanogram amounts of an element (Koornneef et al., 2014). These developments now allow the possibility to study extremely small samples, for example submilligram melt inclusions (Koornneef et al., 2015) and could be applied to dating individual mineral inclusions derived from diamonds. This offers the exploration industry the opportunity to gain a better understanding of the number and timing of diamond forming events within an exploration area providing better assessment of the potential diamond resources.

Compositional characterization of the inclusions is a pre-requisite prior to destructive trace element or isotopic analysis to determine the

* Corresponding author at: Geochemistry department, Research School of Earth Sciences, Australian National University, 142 Mills Road, ACTON 2601, Canberra, Australia.
E-mail address: suzette.timmerman@hotmail.com (S. Timmerman).

http://dx.doi.org/10.1016/j.gexplo.2015.09.016
0375-6742/© 2015 Elsevier B.V. All rights reserved.

number of different inclusion populations in the bulk diamond sample. Determining the number of inclusion populations is of particular importance if inclusions are pooled for isotope analysis, as has been the practice in the past (Richardson et al., 1990; Richardson et al., 1984). Wavelength dispersive (WDS) electron probe microanalysis (EPMA) is the usual characterization method of these inclusions in order to obtain high precision pressure temperature estimates (Cookenboo and Grütter, 2010; Gurney et al., 2005). Traditionally EPMA is performed on polished materials such as thin sections or grain mounts, with a carbon coating to avoid charging effects. The dilemma that is now faced is that the analytical precision of the high precision geochemical techniques required to characterize the isotopic and trace element composition of the inclusions will always be limited by sample size; hence it is desirable to avoid any sample loss by polishing for example.

Here we present a methodology for EPMA of unpolished materials. This method is particularly suitable to inclusions from diamonds as they are frequently characterized by flat crystal surfaces due to the tendency of diamond to impose an octahedral symmetry on inclusions (Meyer, 1987).

Previous electron probe microanalysis of unpolished materials in general showed that X-ray emmissions are highly scattered leading to lower totals (Kielemoes et al., 2000). The density of the sample, fluorescence and the absorbance of radiation can also affect the WDS analysis on unpolished samples. Further, the beam incidence angle and take-off angle and stability of the beam voltage are part of the calculations for quantitative results. Any rough or tilted surface will cause different beam incidence and take-off angles and influence the WDS analysis (Lifshin and Gauvin, 2001). EPMA analysis of porous aluminous catalysts in non-conductive resin resulted in 15 times larger errors and the significant offsets in the major element composition compared to solid samples were attributed to surface contamination and the assumption that the porous sample had the same atomic formula as the solid sample (Sorbier et al., 2004). Signal loss on these porous materials was attributed to charge trapping effects (Sorbier et al., 2000) and not to the direct effect of porosity and roughness as previously argued by Abo-Namous (1989) and Lakis et al. (1992). For porous materials the analyses were corrected with the peak-to-background method, rather than the normal ZAF correction procedure (Abo-Namous, 1989; Statham and Pawley, 1978). The samples had a very high surface roughness and the total concentration of metals often did not exceed 2 wt%. In contrast, as unpolished minerals have total metal concentrations close to 100% and often relatively flat crystal faces, the traditional ZAF correction procedures are more practical than the peak-to-background method. Although wavelength dispersive microanalysis of unpolished solid materials has been previously reported on stainless steel (Kielemoes et al., 2000), two mineral inclusions (Deines and Harris, 2004) and thin sections (Chinner et al., 1969), no detailed method description has been presented and the available data shows only normalized totals for mineral inclusions and 25.6–33.1% totals for stainless steel. Bjärnborg and Schmitz (2013) assessed the quality of energy dispersive (EDS) analysis of unpolished spinel grains by comparison to WDS measurements of polished spinel grains and concluded that it was possible to obtain reliable compositional data, presumably due to spinel having well-defined crystal faces. By comparing the analysis of polished and unpolished samples the uncertainty in the relative trueness of the analysis when utilizing the ZAF correction procedure is common to both analyses and hence cancels out (Pouchou and Pichoir, 1991).

The study presented here investigates the reliability and reproducibility of the more precise WDS technique on unpolished solid silicate minerals with the aim to apply a method to rare 10 to 300 μm mineral inclusions in diamonds, prior to the Rb–Sr and Sm–Nd isotope analysis of the entire grain. In the discussion below, accuracy is used for the trueness of the values and is assessed by comparing it to the analysis of the polished minerals, and precision refers to random errors and includes how well we can repeat the analyses with the same results (reproducibility).

2. Materials and methods

2.1. Materials

Four clinopyroxene (cpx, OR109), four olivine (ol, LE83), and four garnet (grt, LE83) grains from peridotitic xenoliths from the Orapa and Letlhakane diamond mines, Botswana were measured along with the thin sections of these xenoliths. Garnet grains (AT1361) and orthopyroxene, olivine and garnet grains (AT1324) from peridotitic xenoliths from the Venetia diamond mine, South Africa were also analyzed. The number of spot analyses performed on each sample is shown in Table 3. Minerals from mantle xenoliths were chosen as test material as equilibration took place at high temperatures and pressures, leading to a high diffusion rate and consequently minimal major element zonation. Based on this reasoning it is assumed that the unpolished grains and thin sections have an identical major element composition and that they can be compared directly. A second test was performed on euhedral garnet grains from the El Joyazo volcano, Spain, to investigate the effect of sample surface roughness on the results by comparing the success rate and quality of the measurements of euhedral and broken garnets. The flattest surface of the sample was placed perpendicular to the electron beam, so the possibility of a variable take-off angle is minimized. The take-off angle in the standard geometry of the instrument is 40°. The purpose of this study was to validate if unpolished samples can be measured reproducibly and accurately by treating them as polished samples and therefore the take-off angle was not monitored directly.

2.2. Electron probe microanalysis

The minerals were placed on double-sided sticky carbon tape on a glass plate with their flattest faces upwards and carbon coated. Careful sample manipulation is required to ensure that relatively flat sample surfaces are placed perpendicular to the electron beam. Secondary electron imaging was used to select flat surfaces and avoid irregular surfaces (Fig. 1a and b). Each sample consisted of at least 4 grains and each grain was measured at four to five different spots with a beam size of 1 μm with a beam current of 25 nA and an acceleration voltage of 15 kV on the JEOL JXA-8800 M Electron Probe Microanalyzer with 4 spectrometers at the VU University with a set-up according to Table 1. The second test of garnets was performed with a beam size of 1 μm and a beam current of 20 nA and acceleration voltage of 15 kV on the JEOL JXA-8530|F Electron Probe Microanalyzer with 5 spectrometers at the Utrecht University. Peak dwell time was set at 25 s, and each background was set at 12.5 s at the EPMA at the VU University and peak dwell time was set at 30 s (apart from Si, Al, Ca; 20 s) and background at 15 s (Si, Al; 10 s, Ca; 15 s) at the EPMA at Utrecht University. The standards chromite (Cr), corundum (Al), diopside (Si, Ca), fayalite (Fe), ilmenite (Ti), jadeite (Na), NiO (Ni), olivine (Mg), orthoclase (K), and tephroite (Mn) were used. The ZAF correction method was applied to the raw data, with the atomic number (Z) correction of Philibert and Tixier (1968), the absorption (A) correction of Philibert (1963) with the mass absorption coefficients of (Heinrich, 1966) supplied with the PC EPMA JEOL software, and the fluorescence (F) correction of Reed (1965).

3. Results and discussion

3.1. Reproducibility and reliability

Initial analyses on unpolished orthopyroxene, clinopyroxene, garnet, and olivine grains showed that the measurements of clinopyroxenes were extremely consistent with totals generally between 99.1 and 99.7 wt%, while the garnets and olivines more often gave lower totals. Garnet LE83 had 51% of the analyses between 5 and 90 wt%, while garnets AT1361 (9%) and AT1324 (3.5%) had less analyses below 90%. Olivines LE83 and AT1324 had respectively 14% and 37% of

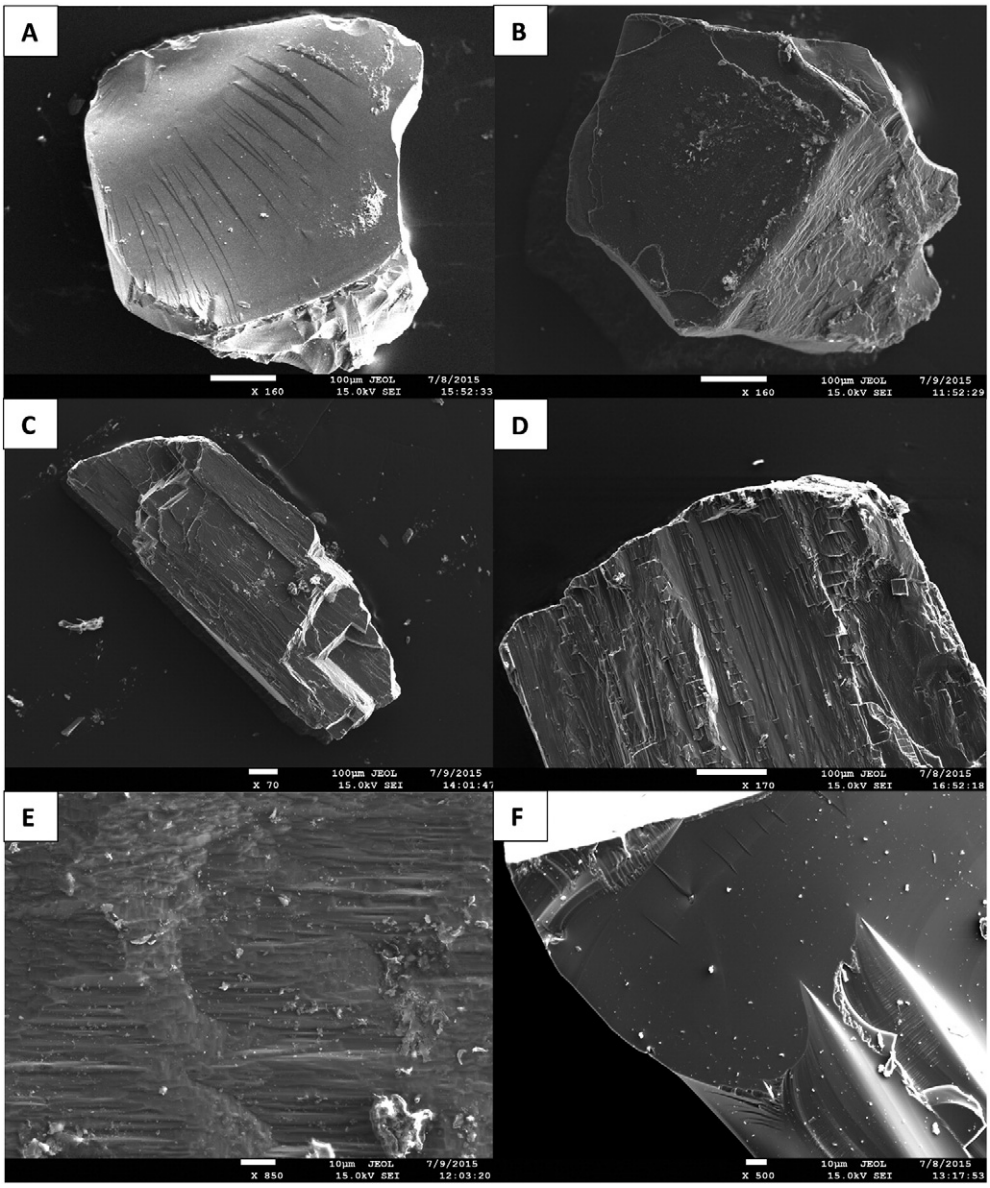

Fig. 1. Secondary electron images of: A) broken garnet of El Joyazo, B) olivine AT1324, C) orthopyroxene AT1324 and D) clinopyroxene MG71 both showing surface relief caused by breakage surface intersecting cleavage planes, E) rough and dusty surface of olivine AT1324, and F) smooth surface of garnet of El Joyazo.

their analyses below 90%. Olivine AT1324 had two grains with all their analyses below 90%, later established to be due to a tilted surface. The low totals were most likely caused by irregular topography or tilted surfaces of the garnets and olivines, compared to the flat surfaces of clinopyroxenes due to strong cleavage and larger crystal faces of the latter (see Fig. 1). Despite the well-developed cleavage and relatively flat faces of the orthopyroxene, the totals are less consistent than the clinopyroxenes. The orthopyroxene grains had 85% of their analyses above 90 wt% total and 61% above 97 wt%.

Table 1
Spectrometer set-up at the VU University and Utrecht University respectively.

Channel	1	2	3	4	1	2	3	4	5
	TAP	TAP	LIF	PETJ	TAP	PETL	PETH	TAPH	LIFH
Crystal	(J)	(J)	(J)	(J)	(J)	(FF)	(FF)	(J)	(FF)
	Na Mg	Si Al	Fe Mn Ni	K Ca Ti Cr	Si Al	Ti Cr	K Ca	Na Mg	Fe Mn Ni

Crystals: TAP: thallium acid phthalate, LIF: lithium fluoride, PET: pentaerythritol, H: high yield spectrometer design with reduced Rowland circle (100 mm), L: large crystal; (J) — Johan analytical crystal design; (FF) — fully focusing Johansson analytical crystal design.

A thorough assessment of the data showed that it was possible to obtain reliable and reproducible results by adopting a rigorous and systematic protocol. As all the minerals under study are anhydrous, analytical totals are expected to be close to 100%, as demonstrated by the thin section analyses. The following protocol was developed: 1) all measurements with totals below 90% were rejected (Fig. 4a and b); 2) the remaining measurements were normalized to a total of 100 wt%; 3) measurements of major elements with concentrations above >2 wt% that were outside 2SD of the average were discarded (Fig. 4c and d); 4) measurements with a magnesium number ($Mg\# = Mg^{2+}/(Mg^{2+} + Fe^{2+})$) outside 2SD were rejected; 5) measurements with a stoichiometry (i.e. ±4 cations per 6O for garnet) outside 2SD were rejected; 6) and finally, the average and the standard deviation of the remaining measurements were calculated (Table 2). Grains with surface contamination or incorrect orientation with respect to the incident electron beam yielded low totals (Fig. 4e and f) and the analyses of these grains were therefore effectively filtered out by step

Table 2
Averages (ave) and 2 standard deviations (2SD) of the major element composition of unpolished orthopyroxene (OPX), clinopyroxene (CPX), garnet (GRT) and olivine (OL) grains and polished thin section determinations (t/s), after rejection of low totals and measurements outside 2SD. *N* represents the number of spots analyzed. BLD is below detection limit, potassium was below detection limit.

		SiO_2	TiO_2	Al_2O_3	Cr_2O_3	FeO	MnO	MgO	CaO	NiO	Na_2O	Total	Mg#	Cations
AT1324 OPX t/s ($n = 6$)	Ave	57.84	bld	1.00	0.41	4.06	bld	36.13	0.33	bld	bld	100.16	94.07	
	2SD	0.68		0.14	0.09	0.12		0.46	0.08			0.97	0.16	
AT1324 OPX grain ($n = 26$)	Ave	56.54	bld	1.12	0.45	4.17	0.10	36.77	0.67	0.10	bld	100.55	94.02	4.03
	2SD	1.66		0.19	0.12	0.33	0.04	1.95	1.20	0.03		5.18	0.59	0.05
AT1361 GRT t/s ($n = 6$)	Ave	42.16	0.22	20.29	4.27	6.31	bld	21.74	4.97	bld	bld	100.12	86.00	
	2SD	0.33	0.06	0.19	0.17	0.13		0.18	0.11			0.41	0.31	
AT1361 GRT grain ($n = 38$)	Ave	39.13	0.19	21.37	4.34	6.33	0.27	23.46	4.86	bld	bld	99.26	86.85	8.15
	2SD	4.10	0.03	1.71	0.25	0.39	0.03	1.89	0.17			4.18	1.05	0.18
AT1324 GRT t/s ($n = 4$)	Ave	42.27	bld	21.81	3.47	6.53	0.40	20.16	5.33	bld	bld	100.70	84.63	
	2SD	0.49		0.21	0.48	0.19	0.10	0.31	0.30			1.02	0.47	
AT1324 GRT grain ($n = 21$)	Ave	43.12	bld	21.71	1.55	8.67	0.38	19.70	4.79	bld	bld	98.84	80.20	4.16
	2SD	1.56		1.26	0.46	0.22	0.04	1.00	0.31			3.28	1.36	0.51
AT1324 OL t/s ($n = 6$)	Ave	41.35	bld	bld	bld	6.51	bld	51.63	bld	0.42	bld	100.67	93.40	
	2SD	0.60			0.02	0.22		0.39		0.03		0.85	0.21	
AT1324 OL grain ($n = 23$)	Ave	38.77	bld	bld	bld	6.80	bld	53.83	bld	0.44	bld	100.69	93.38	2.11
	2SD	2.24			0.02	0.31		2.22		0.04		3.69	0.60	0.10
OR109 CPX t/s ($n = 14$)	Ave	54.50	bld	2.40	0.50	2.14	bld	16.43	22.35	bld	1.51	99.43	93.19	
	2SD	1.30		0.26	0.07	0.44		0.54	0.35		0.12	0.42	0.71	
OR109 CPX grain ($n = 47$)	Ave	54.40	bld	2.59	0.57	2.06	bld	17.21	21.53	bld	1.46	97.93	93.70	4.02
	2SD	2.79		0.51	0.13	0.16		2.28	0.76		0.23	4.29	0.73	0.07
LE83 GRT t/s ($n = 7$)	Ave	41.42	bld	17.96	7.81	6.82	0.38	21.01	4.52	bld	bld	99.15	84.61	
	2SD	0.86		0.35	0.34	0.19	0.05	0.81	0.97			1.26	0.30	
LE83 GRT grain ($n = 10$)	Ave	39.76	bld	18.01	7.54	6.74	0.36	23.33	4.16	bld	bld	98.45	85.87	8.10
	2SD	3.81		1.96	0.58	0.46	0.07	4.05	0.53			4.85	0.85	0.17
LE83 OL t/s ($n = 19$)	Ave	41.19	bld	bld	bld	7.12	bld	51.14	bld	0.39	bld	99.76	92.76	
	2SD	0.78				0.21		0.25		0.06		0.97	0.09	
LE83 OL grain ($n = 24$)	Ave	41.21	bld	bld	bld	7.08	bld	51.15	bld	0.38	bld	98.52	92.69	1.99
	2SD	4.07				0.42		4.22		0.06		6.10	1.02	0.17

1 of the protocol. The rejection of an analysis based on an element being outside 2SD of the data population considered all oxides. In reality this screening was dependent on variation of the major elements that comprised the mineral because minor oxides below 1 wt% have larger relative standard deviations than the major oxides. The data that were rejected were due to major element data outside 2SD of elements that comprised more than 2 wt% of a mineral. The 2SD outlier test assumes that all the analyses have the same composition. Therefore, our methodology is restricted to grains where major element zonation is negligible.

After rejecting the low totals and data that was outside 2 standard deviations, all the major element data of the grains are within error of the thin section results (Table 2, Fig. 3a). The success rate of the measurements varies between the different minerals (Table 3). For clinopyroxene, 73% (47/64) of the measurements remained following the systematic rejection criteria, orthopyroxene had 68% (26/38) acceptable analyses and ~70% of the olivine measurements were accepted (24/35 for LE83 and 32/46 for AT1324 when the tilted grains are neglected), but only 37% (10/27) of LE83 garnet measurements were acceptable. In addition, all the analyses for some grains had totals below 90% either due to a tilted surface or dust (Fig. 1f). This clearly shows the importance of ensuring that grains are flat, perpendicular to the incident beam and cleaned of dust. Garnets AT1361 and AT1324, however, yielded much more reproducible analyses with respectively 84% (38/45) and 72% (21/29) of the analyses being accepted. Therefore, we advise to have a minimum of 20 spot analyses per sample having established that the mineral is orientation is perpendicular to the beam, so there are at least ~8 good analyses to determine a reliable average and 2SD. Following this systematic approach in rejecting some analyses, the mineral data for garnet, olivine, orthopyroxene and clinopyroxene are indistinguishable from the thin section results, Table 2. The only exception is a higher FeO and lower Cr_2O_3 of garnet grain AT1324, leading to an offset in the magnesium number. The relative standard deviation (RSD) of the analyses of unpolished grains is 0.4 to 3.3 times (1.3× on average) higher than the relative standard deviation on the results of the thin sections for the elements minor and trace Na, K, Fe, Mn, Ni, Cr, and Ti. The RSD is 0.6 to 6.2 times higher for the unpolished grains for the major elements Si, Al, and Mg (with the exception of higher RSD for garnet grain AT1361), and 0.6 to 7.8× higher for Ca and an outlier of 16 times higher relative standard deviation for Mg for olivine LE83. In general the RSD on the results of the unpolished grains is similar to the thin sections, showing that the application of the systematic approach on EPMA analyses on unpolished grains is a suitable method to determine the major element compositions reproducibly and accurately. A rigorous assessment of the data reveals that only the average Mg# of garnets LE83 and AT1324 of the unpolished grain is outside 2 standard deviations of the thin section data (Table 2). The magnesium number of the unpolished clinopyroxene is 0.5% higher, olivine 0.02–0.08% lower, and of garnet 1–1.5% higher than the average result of the thin section data (Table 2).

The second test comprised 12 analyses of polished garnets, 109 analyses of unpolished broken surfaces, and 33 analyses of euhedral unbroken crystal faces. This assessment is considered more pertinent to the study of inclusions in diamonds as they are usually characterized by imposed octahedral morphology. This second analytical session produced a higher success rate of measurements (98%) with overall high totals compared to the first test on garnets that only yielded a 40% success rate. When all the measurements are taken into account for the

Table 3
Overview of the number of analyses and number of rejections for each step in the systematic protocol.

	OR109 CPX	AT1324 OPX	LE83 OL	AT1324 OL	LE83 GNT	AT1361 GNT	AT1324 GNT
Original nr of analyses	64	38	35	46	27	45	29
<90%	6	6	5	17	14	4	1
Outside 2SD	7	4	4	3	2	1	4
Mg nr.	3	1	1	2	1	2	1
Stoichiometry	1	1	1	1	0	0	2
Total rejected	17	12	11	23	17	7	8
Remaining analyses	47	26	24	23	10	38	21
Percentage rejected	26.6	31.6	31.4	50	63	15.6	27.6

Table 4
Averages and 2 standard deviations of the major element composition of unpolished euhedral and broken garnet (GRT) grains and their thin section (t/s). All: before rejection of low totals and measurements outside 2SD, sel. (selected): after rejection of low totals and measurements outside 2SD. Na_2O, K_2O, NiO, TiO_2, and Cr_2O_3 were all below detection limit.

	GRT thin sec. ($n = 12$)		GRT euhedral all ($n = 33$)		GRT euhedral sel. ($n = 28$)		GRT broken all ($n = 109$)		GRT broken sel. ($n = 95$)	
	Average	2SD	Average	2SD	Average	2SD	Average	2SD	Average	2SD
SiO_2	36.67	0.28	36.13	2.94	37.51	2.89	36.48	4.91	36.93	3.91
Al_2O_3	20.86	0.38	20.36	1.44	21.06	1.51	20.15	3.6	20.41	2.94
FeO	37.38	0.66	34.33	6.64	35.08	4.64	36.81	2.42	37.17	1.51
MnO	1.13	0.34	1.25	0.54	1.21	0.31	1.34	1.05	1.33	1.01
MgO	3.39	0.15	3.68	1.15	4	0.42	3.27	0.79	3.27	0.62
CaO	0.91	0.12	0.99	0.27	1.07	0.12	0.82	0.16	0.83	0.15
Total	100.37	0.76	96.83	8.19	97.94	3.12	98.93	5.07	99.68	5.92
SiO_2	36.54	0.28	37.34	2.93	38.3	2.95	36.87	4.61	37.04	3.92
Al_2O_3	20.78	0.38	21.04	1.55	21.5	1.54	20.35	3.24	20.47	2.95
FeO	37.25	0.66	35.4	4.98	35.82	4.74	37.22	2.47	37.29	1.52
MnO	1.13	0.34	1.29	0.52	1.23	0.32	1.33	1.09	1.33	1.02
MgO	3.37	0.15	3.81	1.19	4.08	0.43	3.31	0.86	3.28	0.62
CaO	0.91	0.12	1.02	0.27	1.09	0.13	0.83	0.17	0.83	0.15
Total	100		100		100		100		100	

unpolished garnets, it is clear that there is a small offset in silica towards higher values (0.8 wt%) and iron towards lower values (up to 1.8 wt% FeO when measurements are normalized to 100%) compared to the polished garnets, with in general more scatter (higher 2SD) in the broken garnets than in the euhedral garnets (Table 4, Fig. 5a and b), apart from iron (Fig. 5c and d). After rejecting analyses following the systematic approach and normalization to 100%, the data of both broken and euhedral garnets are within error of the results of the thin sections, except for a higher MgO value of the euhedral garnets compared to the thin section. The 2 standard deviations are in general higher for the unpolished garnets than the polished garnets. When the broken garnets are compared to the euhedral garnets, the broken garnets have on average higher totals and less scatter in iron contents, while euhedral garnets have more reproducible silica, alumina, and manganese contents. Surprisingly, the analyses of euhedral garnets were not significantly better than of the broken garnets (Table 4). We interpret this relationship to be due to the surface striations on the crystal faces of the euhedral garnets influencing the measurements (Fig. 2b). The striations had a visible topography of at least ± 10 μm.

The quality of EPMA data of the garnets was also assessed based on five criteria following Locock (2008): the analytical total, proportion of cation sites, presence of octahedral Si, charge balance, and residual total after ascribing garnet end-member components to the analysis. Locock (2008) assigned a quality assessment of superior, excellent, good, fair, and poor dependent on these five criteria. The measurements on the broken garnets mainly had high residual totals between 0.06 and 15.4% and often more than 4%, resulting in a "poor" quality assessment, suggesting that there was difficulty in data acquisition. The conchoidal fractures on the broken garnets could have had an effect on the results (Fig. 2a), as the curved surface will result in different take-off angles for spot analyses in different locations. The residual totals of the euhedral garnets ranged from 0 to 7.1%, with often less than 1%. Taking all criteria into account the measurements of broken garnets had a "fair" quality assessment, while the euhedral garnets had a "good" quality. In general, the results of this second test are in line with the first in that it is possible to obtain reproducible and accurate results of unpolished silicate minerals.

The systematic treatment of the data led to lower standard deviations in the data (Table 2 and 4) and shows that although the precision of measurements on unpolished silicate minerals is not as good as with polished thin sections for all oxides, the results are generally accurate and reproducible. The systematic protocol allows filtering of clear outliers and for this reason the remaining analyses can be statistically treated. When analytical totals were low (50–90 wt%), the aluminum, magnesium, and silicon oxides weight percentages of analysis on unpolished silicate minerals showed an offset up to 67% (MgO garnet) on individual analyses compared with the average thin section results. This observation implies that X-rays produced from the lighter elements such as silica, magnesium, and aluminum that make up a large proportion of the minerals, are more affected by surface topography and Johan geometry of analytical crystals. Calcium, by contrast appears less variable in the unpolished samples (factor of 2.7× greater variance compared to 7.9× for Si). Similarly, the transition metals such as iron and manganese (4.2×, 2.1×), which have a higher mass, also have lower variance than the low mass elements (Table 2). The lighter elements Si, Mg, and Al (1.25–1.74 keV) have a lower X-ray energy than Ca, Mn, and Fe (3.69, 5.90, and 6.40 keV respectively) and since softer X-rays generated at the lower part of the excitation volume are likely to be absorbed by the mineral matrix, Si, Mg, and Al are more easily influenced by surface topography.

A second possible explanation for the offsets in results of Al, Mg and Si is given by the differences in geometry of the spectrometer crystals related to the crystal type, geometry and peak resolution. These elements were measured with TAP crystals that have sharp peaks, while better results of for example Fe, Ca, and Ti were measured on PET and LIF crystals, which have broader peaks. When there is a small shift in the position of the peak, the offset in a sharp peak will have a larger effect than an offset in a broad peak and therefore the latter is less affected

Table 5
Peak shifts in the different spectrometer crystals due to defocusing in steps of 5 μm. The peak intensity measured at 0 (peak position of dZ = 0) is also given.

	TAP		TAPH		LIFL		LIFH		PET	
dZ	Peak pos	Peak at 0	Peak pos	Peak at 0	Peak pos	Peak at 0	Peak pos	Peak at 0	Peak pos	Peak at 0
0	90.675	3393	90.767	3990	134.581	1408	134.827	1676	107.482	767
−5	90.687	3224	90.781	3976	134.583	1369	134.823	1701	107.532	722
−10	90.693	3105	90.796	3883	134.581	1347	134.828	1725	107.537	695
−15	90.709	3030	90.805	3821	134.598	1281	134.833	1680	107.552	631
−20	90.716	2718	90.815	3753	134.614	1256	134.870	1617	107.577	643
−25	90.728	2577	90.836	3562	134.611	1252	134.883	1677	107.542	610
Peak shift	0.053		0.069		0.030		0.056		0.060	

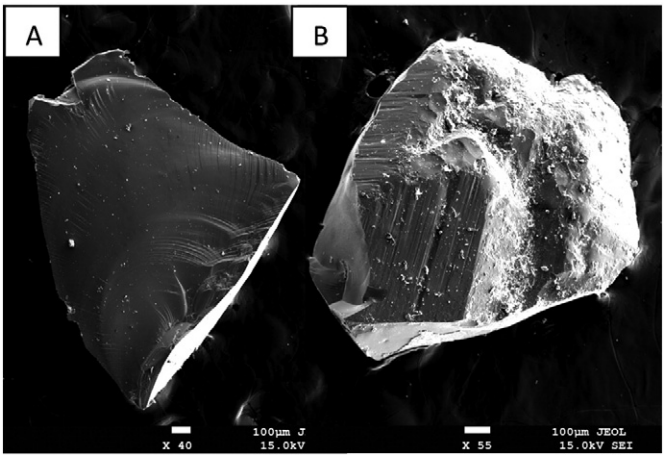

Fig. 2. Secondary electron images of: A) garnet with conchoidal surfaces due to breakage, B) euhedral garnet with flat surfaces and striations caused by differential growth rates, possibly resulting in compositional differences (Fig. 5).

by topography. Advantage of Johansson fully focusing crystal geometry (table 5 with crystal geometries, TAPH and LIFH) is smaller peak shifts due to deviations from the optimal sample position within the Rowland circle because of topography. The Johan crystal geometry is bent to 2× radius of the Rowland circle while the Johansson crystal geometry is ground to the radius of the Rowland circle and allows collection of a signal from a wider range of take-off angles, i.e. less sensitive to defocusing. Such effect can be simulated using measurements of standards at optically displaced positions. Defocusing tests at an offset of −5, −10, −15, −20, and −25 μm were performed with Fe on LIF, Al on TAP and Ca on PET with hematite, corundum and diopside standards. These tests illustrate that the Johan TAP crystals show a larger shift in the peak and measured peak intensities than LIF and PET crystals, particularly those with Johansson design (Fig. 6, Table 5).

In addition, the quality of the results can be dependent on the absorption coefficient and X-ray energy specific for an element. We only consider the Kα lines here. The absorption correction (*A*) is more important due to different values, i.e. 1.8 for Na and 1 for Ca, compared to the *Z* and *F* corrections which are very similar for each element. Calcium for example has a high X-ray energy and thus a stronger radiation, causing larger excitation volume of the sample. Sodium has a lower X-ray energy and hence has a smaller excitation volume. The mass absorption coefficient increases when the X-ray energy line decreases and the effect of topography is for this reason more pronounced for measured lower energy X-ray lines. The data show this relationship semi-quantitatively (Fig. 3b). The combination of factors described above (i.e. crystal geometry, topography, spectral resolution) results in calcium being less influenced by topography than sodium and leading to better reproducibility for Ca (Table 2). Previous work by Markowicz and Van Grieken (1984) also found a large deviation (50%) for low-Z elements for analysis on samples with curved surfaces and submicrometer particles that they attributed to the curvature of the samples. They proposed expressions to correct analysis of curved samples but suggested that for materials comprising elements of similar atomic numbers that the peak-to-background and ZAF correction approach should produce correct data. Some of the offsets in the analysis compared to "true" values observed in our study, appears, however, to be explained by their rough or inclined surface. Despite a flat surface, a tilt in the surface relative to the beam would lead to a different beam incidence angle and take-off angle. Lifshin and Gauvin (2001) demonstrated that a change in beam incidence angle of 10° results in a change in X-ray intensity of <2%, while a change in the take-off angle of 5° can lead to a relative shift of 8% for Al and <1% for Ni. Although quantitative analyses are obtained under a normal (90°) beam incidence angle, a different beam angle does not have a large effect. In contrast the take-off angle is much more important and will be altered differently for each spectrometer and element (Tsuji et al., 1999), with a larger effect for the lower X-ray energy elements (Lifshin and Gauvin, 2001). The rough surface (striations, dust and topography) can lead to intensity discrepancies (Gauvin and Lifshin, 1999) due to different take-off angles. The take-off angle is different for each element as the surface tilt relative to the position of each spectrometer is specific. Any tilting caused by striations, dust and topography thus changes the take-off angle of each element to different extents. The effect of a different take-off angle seems to be present in Si, Al, and Mg in some of the analyses, but due to their offset compared to the average of all the analysis, these outliers are rejected by the data assessment procedure.

The study presented here demonstrates that the analysis of flat mineral surfaces and data normalization to 100% leads to reliable and reproducible results, especially for elements with a relative atomic number mass > Ca (>30 g/mol or *Z* > 20) i.e. the range of elements for which concentration can be measured using Ka emission lines at typical conditions of EPMA (15–20 kV). A notable proviso of this conclusion is that mineral grains need to be small enough to be within the focus range of the EPMA when using glass plates at normal stage height. In this study, all the minerals of the first test were similar in size (~0.7 mm) and the garnets from the second test were lower in height (~0.4 mm). Although focusing on rough grains is more difficult than on polished samples, in general there were no major difficulties in obtaining optimal focal positions and no sample height adjustment was needed. In the case of grains larger than ~1 mm, charging effects can start to occur and different mounting options such as imbedding into indium have to be used. Further, extra coating such as C paint can help to avoid charging effects. For further geochemical analysis of the grains after EPMA analyses, the carbon coating can be removed by a gentle wash with ethanol. Other coatings

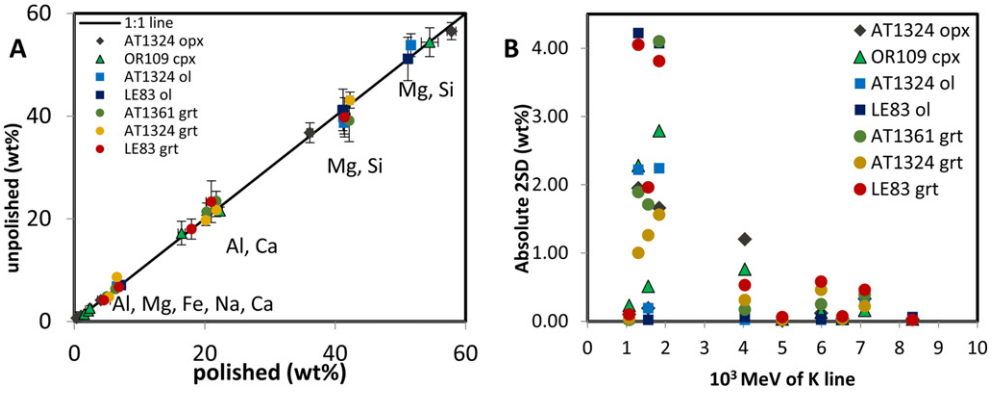

Fig. 3. A) Illustration of the major element compositional deviation between the unpolished samples and the polished samples. B) Variability in 2SD compared to the X-ray energy of the Kα line of each element.

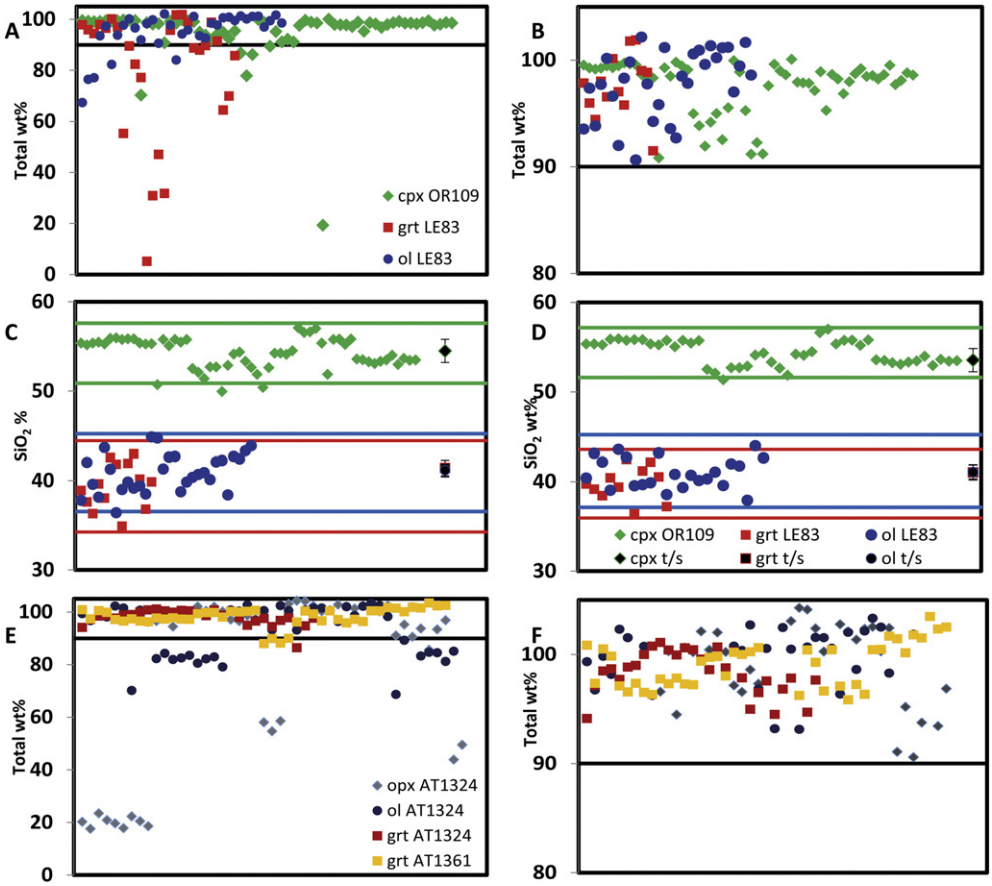

Fig. 4. A) Total wt% of each analysis on unpolished clinopyroxene OR109, garnet, and olivine grains LE83, B) measurements with a total of >90 wt%, C) silica content in unpolished clinopyroxene, orthopyroxene, garnet, and olivine grains with totals above >90 wt% (right side: average of thin sections), D) silica content of unpolished clinopyroxene, garnet, and olivine grains after rejection of measurements with major element compositions, Mg number and stoichiometry outside 2SD. t/s is the abbreviation for thin section and the green (cpx), blue (olivine) and red (garnet) dashed lines represent the 2SD in Figures C and D. Graphs C and D are on the same scale showing clearly the improvement in the quality of the data after rejection of outliers. E) Total wt% of orthopyroxene, olivine and garnet grains from sample AT1324 and garnet grains from AT1361, this figure clearly shows the tilted grains and dusty grains of which all the analyses were below 90% for two orthopyroxene and two olivine grains (multiple spots). F) Analyses remaining after rejection of totals below 90 wt%.

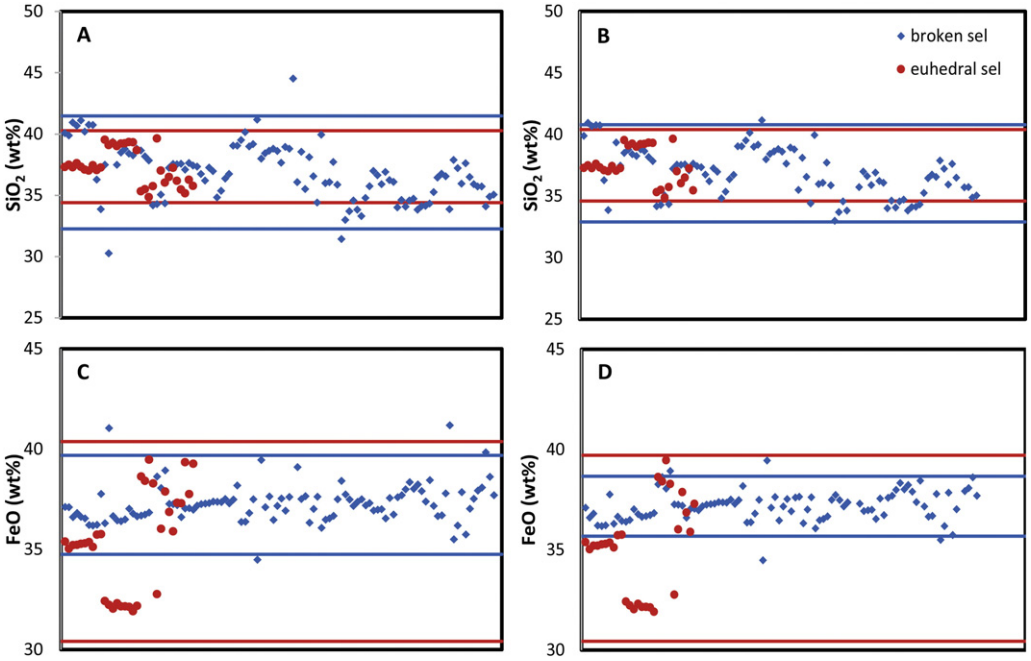

Fig. 5. A) silica content of all the analyses of the broken (blue) and euhedral (red) garnets, B) silica content of the analyses after rejection of outliers for the broken and euhedral garnets, C) iron content of all the analyses of the broken (blue) and euhedral (red) garnets, D) iron content of the analyses after rejection of analyses for the broken and euhedral garnets. The lines represent the 2SD.

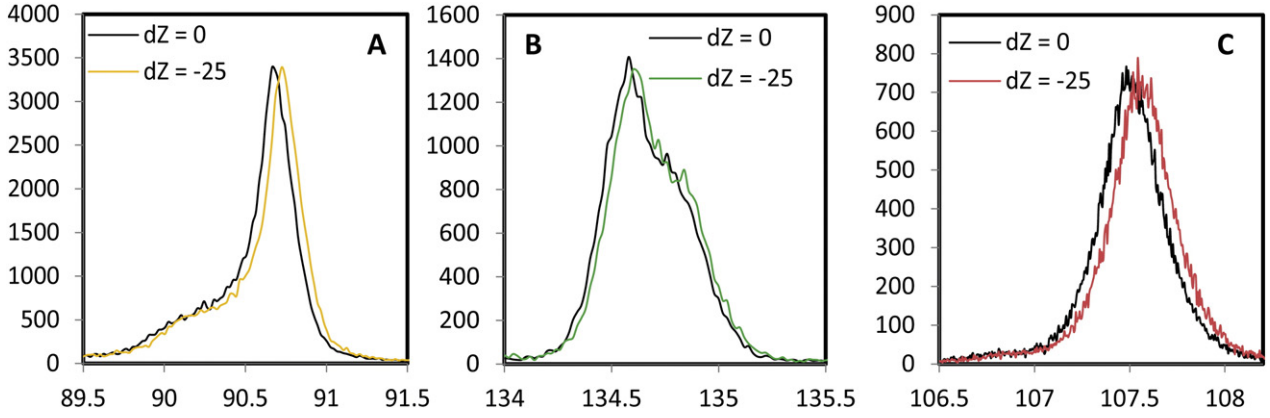

Fig. 6. Illustration of the peak shift between $Z = 0$ and defocused at $dZ = -25$ μm for TAP (a), LIFL (b) and PET (c) crystals. All tests were performed at 15 kV and 15 nA, and 1 μm beam size. Qualitative WDS scans were acquired on corundum (TAP, AlKa), hematite (LIF, FeKa) and diopside (PET, CaKa) standards. Spectrometer step size was 20 μm and dwell time 200 ms/step. Measurements were done at optical focus position (chosen as mean value of 3 automatic focus searches) and 5 defocused positions: $dZ = -5, -10, -15, -20$, and -25 μm. The *y*-axis represents the intensity of the signal; the *x*-axis is the wavelength of the specific element measured on each crystal.

like Au, Ag, or Pt could be used, but the removal of these coatings with a KSO_4 solution could be more harmful to the samples.

3.2. Applications

This study has shown that filtering of EPMA data of unpolished silicate minerals can produce accurate and reproducible results. The approach is especially applicable for minerals with euhedral flat crystal surfaces. This method therefore is ideal for the analysis of rare and unique samples when the sample cannot be destroyed or all the material is required for trace element and isotope analysis, i.e., cannot be reduced by polishing. Notable potential applications include minerals from rare or unique samples (e.g. meteorites, archaeological artefacts and mineral inclusions in diamonds). In the context of diamond exploration, determining the geothermal gradient beneath a potential diamond mine is of vital importance to establishing the depth range over which diamonds can be sampled by the host volcanic rocks. This is usually determined using indicator mineral but inclusions in diamonds provide important additional constraints. An advantage of inclusions in diamonds is their flat surfaces due to their imposed cubic-octahedral morphology. In addition, a practical advantage is that these mineral inclusions are larger than the beam diameter of the EPMA, but small enough to be within the optical focal range while mounted on conventional thin section surface (<500 μm).

4. Conclusions

EPMA analyses of unpolished and polished garnets, clinopyroxenes, orthopyroxenes and olivines demonstrate that it is possible to measure unpolished silicate minerals with reliable and reproducible results when the systematic data evaluation protocol is followed. This approach is proposed for the major element characterization of small rare or unique mineral grains that can subsequently be subjected to analytical geochemistry techniques. Our treatment of analytical results allows to identify unpolished mineral grains can be treated as regular polished samples. In such case there is great potential for application of the technique to the study of inclusions in diamonds allowing both the geothermal gradient to be defined at the time of diamond formation as well as allowing geochronology to later determine the time of diamond formation.

Acknowledgements

We thank Sharon de Jong for providing unpublished data of the thin sections of the samples for the first test. The VU University Amsterdam funded this research. We are extremely grateful for the input of 2 anonymous reviewers and editor Robert Ayuso for the constructive criticism and efficient editorial handling.

References

Abo-Namous, S., 1989. On the peak-to-background ratio in microprobe analysis of porous materials. Microbeam Analysis, pp. 239–241.
Averill, S.A., 2001. The application of heavy indicator mineralogy in mineral exploration with emphasis on base metal indicators in glaciated metamorphic and plutonic terrains. Geol. Soc. Lond., Spec. Publ. 185 (1), 69–81.
Bjärnborg, K., Schmitz, B., 2013. Large spinel grains in a CM chondrite (acfer 331): implications for reconstructions of ancient meteorite fluxes. Meteorit. Planet. Sci. 48 (2), 180–194.
Chinner, G., Smith, J., Knowles, C., 1969. Transition-metal contents of Al2SiO5 polymorphs. Am. J. Sci. A 267, 96–113.
Coker, W.B., 2010. Future research directions in exploration geochemistry. Geochem. Explor. Environ. Anal. 10 (1), 75–80.
Cookenboo, H.O., Grütter, H.S., 2010. Mantle-derived indicator mineral compositions as applied to diamond exploration. Geochem. Explor. Environ. Anal. 10 (1), 81–95.
Deines, P., Harris, J., 2004. New insights into the occurrence of 13 C-depleted carbon in the mantle from two closely associated kimberlites: Letlhakane and Orapa, Botswana. Lithos 77 (1), 125–142.
Gauvin, R., Lifshin, E., 1999. Electron backscattering profile of rough surfaces. Scanning 21 (2), 144–145.
Griffin, W.L., Ryan, C.G., 1995. Trace elements in indicator minerals: area selection and target evaluation in diamond exploration. J. Geochem. Explor. 53 (1–3), 311–337.
Grütter, H.S., Gurney, J.J., Menzies, A.H., Winter, F., 2004. An updated classification scheme for mantle-derived garnet, for use by diamond explorers. Lithos 77 (1–4), 841–857.
Gurney, J.J., Helmstaedt, H., Le Roex, A., Nowicki, T., Richardson, S., Westerlund, K., 2005. Diamonds: crustal distribution and formation processes in time and space and an integrated deposit model. Econ. Geol. 100, 143–177.
Heinrich, K.F., 1966. X-ray absorption uncertainty. The Electron Microprobe, pp. 296–377.
Kielemoes, J., Hammes, F., Verstraete, W., 2000. Measurement of microbial colonisation of two types of stainless steel. Environ. Technol. 21 (7), 831–843.
Koornneef, J.M., Bouman, C., Schwieters, J.B., Davies, G.R., 2014. Measurement of small ion beams by thermal ionisation mass spectrometry using new 10^13Ohm resistors. Anal. Chim. Acta 819, 49–55.
Koornneef, J.M., Nikogosian, I., van Bergen, M.J., Smeets, R., Bouman, C., Davies, G.R., 2015. TIMS analysis of Sr and Nd isotopes in melt inclusions from Italian potassium-rich lavas using prototype 10^13Ω amplifiers. Chem. Geol. 397, 14–23.
Lakis, R., Lyman, C., Goldstein, J., 1992. Electron-probe microanalysis of porous materials. Proceedings of the annual meeting — Electron Microscopy Society of America. San Fransisco Press, p. 1660.
Lifshin, E., Gauvin, R., 2001. Minimizing errors in electron microprobe analysis. Microsc. Microanal. 7 (02), 168–177.
Locock, A.J., 2008. An excel spreadsheet to recast analyses of garnet into end-member components, and a synopsis of the crystal chemistry of natural silicate garnets. Comput. Geosci. 34 (12), 1769–1780.
Macnae, J., 1979. Kimberlites and exploration geophysics. Geophysics 44 (8), 1395–1416.
Markowicz, A.A., Van Grieken, R.E., 1984. Composition dependence of bremsstrahlung background in electron-probe X-ray microanalysis. Anal. Chem. 56 (12), 2049–2051.
Meyer, H., 1987. Inclusions in diamond. Mantle Xenoliths, pp. 501–522.
Philibert, J., 1963. A method for calculating the absorption correction in electron probe microanalysis. X-ray Optics and X-ray Microanalysis, pp. 379–392.
Philibert, J., Tixier, R., 1968. Electron penetration and the atomic number correction in electron probe microanalysis. J. Phys. D. Appl. Phys. 1 (6), 685.
Pouchou, J.-L., Pichoir, F., 1991. Quantitative analysis of homogeneous or stratified microvolumes applying the model "PAP". Electron Probe Quantitation 31-75. Springer.

Reed, S., 1965. Characteristic fluorescence corrections in electron-probe microanalysis. Br. J. Appl. Phys. 16 (7), 913.
Richardson, S.H., Erlank, A.J., Harris, J.W., Hart, S.R., 1990. Eclogitic diamonds of proterozoic age from cretaceous kimberlites. Nature 346 (6279), 54–56.
Richardson, S.H., Gurney, J.J., Erlank, A.J., Harris, J.W., 1984. Origin of diamonds in old enriched mantle. Nature 310 (5974), 198–202.
Sorbier, L., Rosenberg, E., Merlet, C., 2004. Microanalysis of porous materials. Microsc. Microanal. 10 (06), 745–752.
Sorbier, L., Rosenberg, E., Merlet, C., Llovet, X., 2000. EPMA of porous media: a Monte Carlo approach. Microchim. Acta 132 (2–4), 189–199.
Statham, P., Pawley, J., 1978. New Method for Particle X-Ray Micro-Analysis Based on Peak to Background Measurements. Scanning electron microscopy vol. I.
Tsuji, K., Wagatsuma, K., Nullens, R., Van Grieken, R.E., 1999. Grazing exit electron probe microanalysis for surface and particle analysis. Anal. Chem. 71 (13), 2497–2501.